Geophysical Research Letters

RESEARCH LETTER
10.1029/2019GL086500

Azimuthal Variation of Magnetopause Reconnection at Scales Below an Earth Radius

Ying Zou[1], Brian M. Walsh[2], Emil Atz[2], Haoming Liang[3], Qianli Ma[4,5], and Vassilis Angelopoulos[6]

[1]Department of Space Science, University of Alabama in Huntsville, Huntsville, AL, USA, [2]Department of Mechanical Engineering and Center for Space Physics, Boston University, Boston, MA, USA, [3]Department of Physics and Astronomy, West Virginia University, Morgantown, WV, USA, [4]Department of Astronomy and Center for Space Physics, Boston University, Boston, MA, USA, [5]Department of Atmospheric and Oceanic Sciences, University of California, Los Angeles, CA, USA, [6]Department of Earth, Planetary and Space Sciences, University of California, Los Angeles, CA, USA

Abstract While magnetopause reconnection naturally occurs in three-dimensional environments, our understanding of the process has been mainly confined to the two-dimensional reconnection plane. How reconnection varies in the third direction, that is, the azimuthal direction, and what causes the variation remain open questions. We study the azimuthal variation of reconnection at an underexplored scale, which is below an Earth radius, using THEMIS spacecraft. Our results show that reconnection jets transition from being present to absent within tenths of a R_E, corresponding to tens of ion inertial lengths. The absence of jets cannot be explained by an ion or electron diffusion region, or a magnetic flux rope flanked by two reconnection sites. The sharp transition of reconnection is associated with spatially varying waves. No drivers of the transition are identified locally at the magnetopause or in the upstream, implying that reconnection may naturally have a finite extent at certain stages of its development.

Plain Language Summary Magnetic reconnection extracts energy from the solar wind to power plasma convection, auroral displays, and geomagnetic substorms and storms in Earth's magnetosphere. Although reconnection is often pictured as a two-dimensional laminar process, where oppositely directed magnetic field lines in a plasma break and reconnect, the actual reconnection is three-dimensional where it varies along the direction perpendicular to the plane. Since the scale in the third dimension determines how much energy is imparted to the magnetosphere, knowledge of how reconnection varies in this direction and what causes the variation is extremely important. Among existing reports, the utilized spacecraft constellations are often too small or too large, only loosely constraining the range of variability in the third dimension. Here, we use serendipitous constellations with a spatial size that is right at the predicted scale for reconnection to vary. Our results show that reconnection jets transition from being present to absent within tenths of an Earth radius. The sharp transition of reconnection is associated with spatially varying waves. Causes of the transition cannot be identified from the surrounding or upstream electromagnetic field and plasma conditions, implying that reconnection may naturally have a finite extent at certain stages of its development.

Key Points:
1. We study the azimuthal variation of magnetopause reconnection at sub-R_E scale using serendipitous THEMIS constellations
2. Reconnection jets transition from present to absent within tens of ion inertial lengths, in association with spatially varying waves
3. We do not observe clear drivers of the finiteness of reconnection locally at the magnetopause or in the upstream magnetosheath

Supporting Information:
- Supporting Information S1

Correspondence to:
Y. Zou,
yz0025@uah.edu

Citation:
Zou, Y., Walsh, B. M., Atz, E., Liang, H., Ma, Q., & Angelopoulos, V. (2020). Azimuthal variation of magnetopause reconnection at scales below an Earth radius. *Geophysical Research Letters*, *47*, e2019GL086500. https://doi.org/10.1029/2019GL086500

Received 3 DEC 2019
Accepted 5 FEB 2020
Accepted article online 7 FEB 2020

1. Introduction

The structure of magnetic reconnection in the direction of the X-line has yet been well understood. At Earth's magnetopause and under a southward interplanetary magnetic field (IMF), the direction typically corresponds to the azimuthal direction, or local time. Limited understanding has been acquired about how reconnection varies in this direction and what causes the variation, although the knowledge would be critical to understand how much energy from the solar wind enters Earth's magnetosphere. A common approach is to survey reconnection at spacecraft separated by various distances and examine whether and how much the process differs. Using this method, studies have derived presence of null structures in the magnetic field (Chen *et al.,* 2017; 2019; Fu *et al.,* 2015; 2017; 2019a; Wang *et al.,* 2019). We focus on situations where, according to reconnection signatures (e.g., reconnection jets), reconnection is present at one point and absent at another and study the transition from presence to absence.

At kinetic scales, signatures of reconnection are often simultaneously observed by spacecraft separated by tens of kilometers (e.g.,Burch *et al.,* 2016 ; Burch & Phan, 2016 ; Chen *et al.,* 2016 ; Genestreti *et al.,* 2017,

2018 ; Phan *et al.,* 2016 ; Torbert *et al.,* 2017). On large scales of a few to >10 Earth radius (R_E), the signatures are sometimes simultaneously observed at multiple spacecraft (e.g.,Dunlop *et al.,* 2011 ; Hasegawa *et al.,* 2016 ; Phan *et al.,* 2000; 2006), sometimes by one spacecraft only (e.g.,Fear *et al.,* 2010 ; Walsh *et al.,* 2017 ; Zou *et al.,* 2019). The former indicates that reconnection spans a few and >10 R_E, either as a continuous X-line or a group of discontinuous patches. The latter suggests that reconnection transition from presence to absence at a-few-R_E scale, although it is uncertain whether this scale reflects the true scale of variation or merely gives an upper bound because of the spatial resolution of the observations offered by the spacecraft separation.

Whether reconnection varies between the kinetic and a-few-R_E scales has been less investigated. This scale is referred to as the sub-R_E scale in this paper, which corresponds to a few to tens of ion inertial lengths under typical magnetosheath conditions (Cassak & Fuselier, 2015) (electron inertial lengths are also <1 R_E, but we only focus on the ion scales). Various three-dimensional simulations in rectangular geometry have shown, based on the strength of the reconnected magnetic field and the reconnection exhausts, that it is at the ion scales that reconnection transitions from being active to the inactive background current sheet (Liu *et al.,* 2019; Nakamura *et al.,* 2012; Shay *et al.,* 2003; Shepherd & Cassak, 2012). Shay *et al*. (2003), Meyer (2015), and Liu *et al*. (2019), using simulations, further propose that the minimum azimuthal scale of reconnection is about ten ion inertial lengths. Testing these models has been challenging due to the lack of spacecraft observations from constellations or serendipitous conjunctions at sub-R_E scales. Multi-spacecraft measurements during the first few years of the CLUSTER mission reveal that magnetic flux structures produced by transient magnetopause reconnection, that is, flux transfer events, commonly (70%) do not extend across the whole constellation (<1 R_E) (Wang *et al.,* 2005), implying that the sub-R_E scale is a critical azimuthal scale for magnetopause reconnection.

What causes reconnection to be active at one region and absent at another remains an open question. One possibility is that only a portion of the current sheet layer meets the threshold for reconnection onset. Reconnection occurrence has been found to depend on local conditions of the current layer, including magnetic shear angle and plasma β (Paschmann *et al.,* 1986; Phan *et al.,* 2013; Scurry *et al.,* 1994; Swisdak *et al.,* 2003; 2010), plasma density (Borovsky *et al.,* 2008; Walsh *et al.,* 2014a; 2014b), velocity shear (Cassak & Otto, 2011; Liu *et al.,* 2018), current sheet thickness (Xu *et al.,* 2018; Liu *et al.,* 2019; Fu *et al.,* 2019b; Li *et al.,* 2020), and upstream inflow velocity (Fu *et al.,* 2013b; 2013a). Reconnection is also affected by the upstream driving conditions. If convection toward the reconnecting current sheet is localized, reconnection will be localized (Pritchett & Coroniti, 2001). Another possibility is that reconnection is an intrinsically patchy process in space (Kan, 1988; Nishida, 1989).

2. Methodology

We study how reconnection varies in the azimuthal direction at the sub-R_E scale and whether the variation is driven by local magnetopause and upstream magnetosheath conditions. We select constellations formed by THEMIS spacecraft that crossed the magnetopause <1 min apart near the subsolar region and are separated by <1 R_E in the Y direction of geocentric solar magnetospheric (GSM) coordinate. The <1-min separation is regarded as being simultaneous enough for this study because previous studies have found that reconnection often turns on and off on a time scale of >2 min (Fasel, 1995; Kuo *et al.,* 1995; McWilliams *et al.,* 2000). As seen below, the actual separation between successive magnetopause crossings varies from a few to 20 s. Although there also exists evidence that reconnection varies on a time scale of a few seconds (Fu, Cao, *et al.,* 2013a; Fu, Cao, *et al.,* 2019a; Fu, Khotyaintsev, *et al.,* 2013b), the reconnection signatures in our selected events persisted tens of seconds up to 1 min as the spacecraft crossed the magnetopause, indicating that the reconnection events under analysis were active at least for this duration.

The required constellations were common in the dayside science phase in Fall 2010, during which they were constituted of THA, THD, and THE. We additionally require that there is a clear magnetic field rotation at the magnetopause, and survey situations when at least one but not all spacecraft observe reconnection jets. Availability of burst-mode data is preferred. Three events are identified and presented in this paper.

Active reconnection is identified based on reconnection ion jets that are consistent with the Walén relation (Hudson, 1970; Paschmann *et al.,* 1979), although we also investigate whether the spacecraft has passed the

ion diffusion region (IDR) and electron diffusion region (EDR) as shown below. The Walén test is conducted following Phan & Paschmann (1996); Phan *et al*. (2013), Trenchi *et al*. (2008), and Zou *et al*. (2019). Briefly, we compare the maximum ion bulk velocity change across the magnetopause $\Delta \boldsymbol{V}$ obtained from observations and Walén prediction. The predicted velocity change is

$$\Delta \boldsymbol{V}_{\mathbf{predict}} = \pm(1-\alpha_1)^{1/2}(\mu_o\rho_1)^{-1/2}[\boldsymbol{B_2}(1-\alpha_2)/(1-\alpha_1)-\boldsymbol{B_1}], \quad (1)$$

where $\boldsymbol{B}$ and ρ are the magnetic field vector and plasma mass density, μ_0 is the vacuum permeability, and $\alpha = (p_{||} - p_{\perp})\mu_0/B^2$ is the anisotropy factor where $p_{||}$and $p_{\perp}$ are the plasma pressures parallel and perpendicular to the magnetic field. The subscripts 1 and 2 refer to a 10-s reference interval in the magnetosheath and to a point within the magnetopause, respectively. If $\Delta V^* = \left(\Delta \boldsymbol{V}_{\mathbf{observe}} \cdot \Delta \boldsymbol{V}_{\mathbf{predict}}\right) \Big/ \left|\Delta \boldsymbol{V}_{\mathbf{predict}}\right|^2 > 0.5$, the agreement is regarded to be significant, which implies that the observed ion bulk flow is a result of reconnection acceleration.

3. Observations

3.1. Spatial Variation of Reconnection

Figure 1 presents the locations of the three spacecraft for the three studied events in the GSM Y-Z plane. The spacecraft observing reconnection jets are denoted by solid circles and those not observing by open circles. As seen from Figures 1a–1c, THE was positioned duskward of THA by only 0.1–0.2 R_E, and THD was duskward of THE by 0.4–0.5 R_E for each event, which translates to 9–30 and 37–86 ion inertial lengths based on the observed magnetosheath conditions (magnetosheath conditions shown below). Zooming out to the global scale, Figures 1d–1f present the spacecraft location in the context of magnetic shear angle distribution along the dayside magnetopause. The shear angle is calculated following Trattner *et al*. (2007). The ridge of maximum magnetic shear is marked with white curves, and it signifies the most probable location for reconnection to occur within the model (Trattner *et al.,* 2007). The three spacecraft (marked as blue dots), whose locations became indistinguishable given the large axis ranges of this figure, were positioned <2 R_E away from the X-line of component reconnection in all events.

3.1.1. Event #1

Figure 2 presents in situ magnetopause measurements on 27 September 2010. Panels a1–a4, b1–b4, and c1–c4 present the magnetic field, plasma density, ion energy spectra, and ion bulk velocity at THA, THE, and THD during the same 90-s interval. The magnetic field and velocity are presented in *LMN* coordinates, which are determined by minimum variance analysis (MVA) of each spacecraft data. The projection of *N* direction was (0.922, −0.386, −0.005), (0.950, −0.296, −0.094), and (0.951, −0.303, −0.063) in GSM coordinates for THA, THE, and THD, respectively. The magnetopause current sheet is shaded in pink, and this is where we look for signatures of reconnection. THD observed an ion bulk flow with a peak speed of 357 km/s (panel c4). For reference, the hybrid Alfvén speed was 351 km/s. This means that the flow at THD was Alfvénic, providing strong evidence that reconnection was active at the THD longitude. A Walén test reveals that the observed reconnection jet speed was 86% of the predicted speed and that the direction differed from the predicted jet by 15°. ΔV^* was 0.83, confirming that THD observed a reconnection jet.

THE also detected a reconnection jet, as the ion bulk flow speed at the magnetopause (Panel b4) was 77% of the predicted speed, and the flow direction differed from the prediction by 24°. ΔV^* was 0.71. On the other hand, no reconnection jet was measured at THA as the ion bulk flow speed was below the Alfvén speed (panel a4) and ΔV^* was only 0.39. One interesting feature is that ΔV^*dropped from the most duskward-located THD to the most dawnward-located THA. Similarly monotonic trends are found in the following two events, suggesting that reconnection jets downstream of the X-line subside gradually from the reconnection site to the surrounding nonreconnecting current sheet.

Could reconnection still be active at THA? One possibility is that THA crossed the IDR or EDR where the Walén relation is not expected to be satisfied. To discern IDRs, we compare the perpendicular plasma bulk velocity and the electric field drift velocity $\frac{E\times B}{|B|^2}$ in the GSM Z direction since $E+V\times B = 0$ does not hold in IDRs. The choice of the Z direction is because it roughly marks the expected direction of the $E \times B$ drift arising from the reconnection electric field E_M, and previously identified IDRs showed a large departure of ion

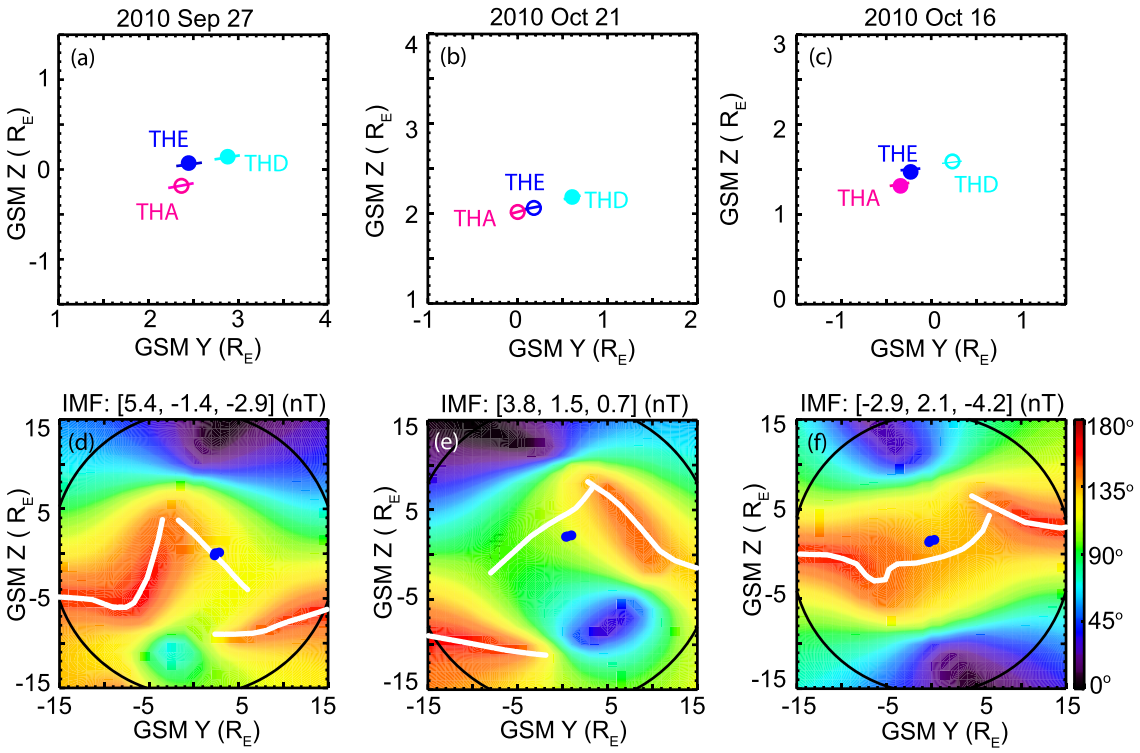

Figure 1. (a–c) Spacecraft location in GSM Y-Z plane. The spacecraft observing reconnection jets are denoted by solid circles and those not observing by open circles. (d–f) Spacecraft location (blue dots) in the context of the magnetopause shear angle as viewed from the Sun. The shear angles were calculated with the magnetic field direction of the T96 model and the draped IMF conditions at the magnetopause. The IMF conditions were taken as 10-min averaged OMNI solar wind data and are marked on top of each panel. Locations of maximum shear angles are marked by the white curve. The black circle represents the size of the magnetopause at the terminator.

bulk flows from the $E \times B$ drift in this direction (e.g.,Dai *et al.,* 2015 ; Mozer *et al.,* 2002). The two velocities are presented in panel a5, and they have shown good consistency. The slight difference (tens of kilometers per second) is interpreted to lie within the error bar because a similar difference is observed in the magnetosheath, where the two velocities are expected to be the same. Signatures of EDRs include large parallel electric fields, intense currents, fast electron bulk flows, and strong electron heating (Burch *et al.,* 2016). Using THEMIS measurements, Tang *et al.* (2013) identified an EDR based on electron bulk velocity and temperature, where the temperature shows large anisotropy of >7 and strong heating of >150 eV. The electron temperature is presented in panel a6, and it is not consistent with EDRs. Unfortunately, limited by time resolution, THEMIS cannot identify EDRs finer than 3 s (Cao *et al.,* 2017).

Another possibility is that THA passed a magnetic flux robe flanked by two active reconnection X-lines. If true, we expect an increase in the total magnetic field as in Øieroset *et al*. (2014), which is again not observed in panel a1.

Hence, the available evidence suggests that reconnection has transitioned from being active at THD and THE to being inactive at THA. We interpret the transition as occurring mainly in the azimuthal direction, as opposed to the GSM Z direction, because reconnection jets are mostly directed in the GSM Z direction, and if not decelerated by other processes, they can extend a few R_E, if not longer, from the X-line (e.g.,Trattner *et al.,* 2012 ; 2018). The spacecraft configuration is not consistent with reconnection jets being decelerated because THA was located upstream, rather than downstream, of the reconnection jets seen by THD and THE.

We present spectrograms of electric fields E_w and magnetic fields B_w in the spacecraft spin plane at THD in panels c7–c10. The ratio of E_w to B_w is also calculated and displayed in panel c11. Considering that the ratio increases with wave normal angle for waves at a given frequency (Figure S1 in the supporting information), we use it as a proxy of the wave normal angle. At low frequencies, THD observed broad electromagnetic wave enhancement below ~200 Hz. The bulk of B_w power spectral density were around and below the

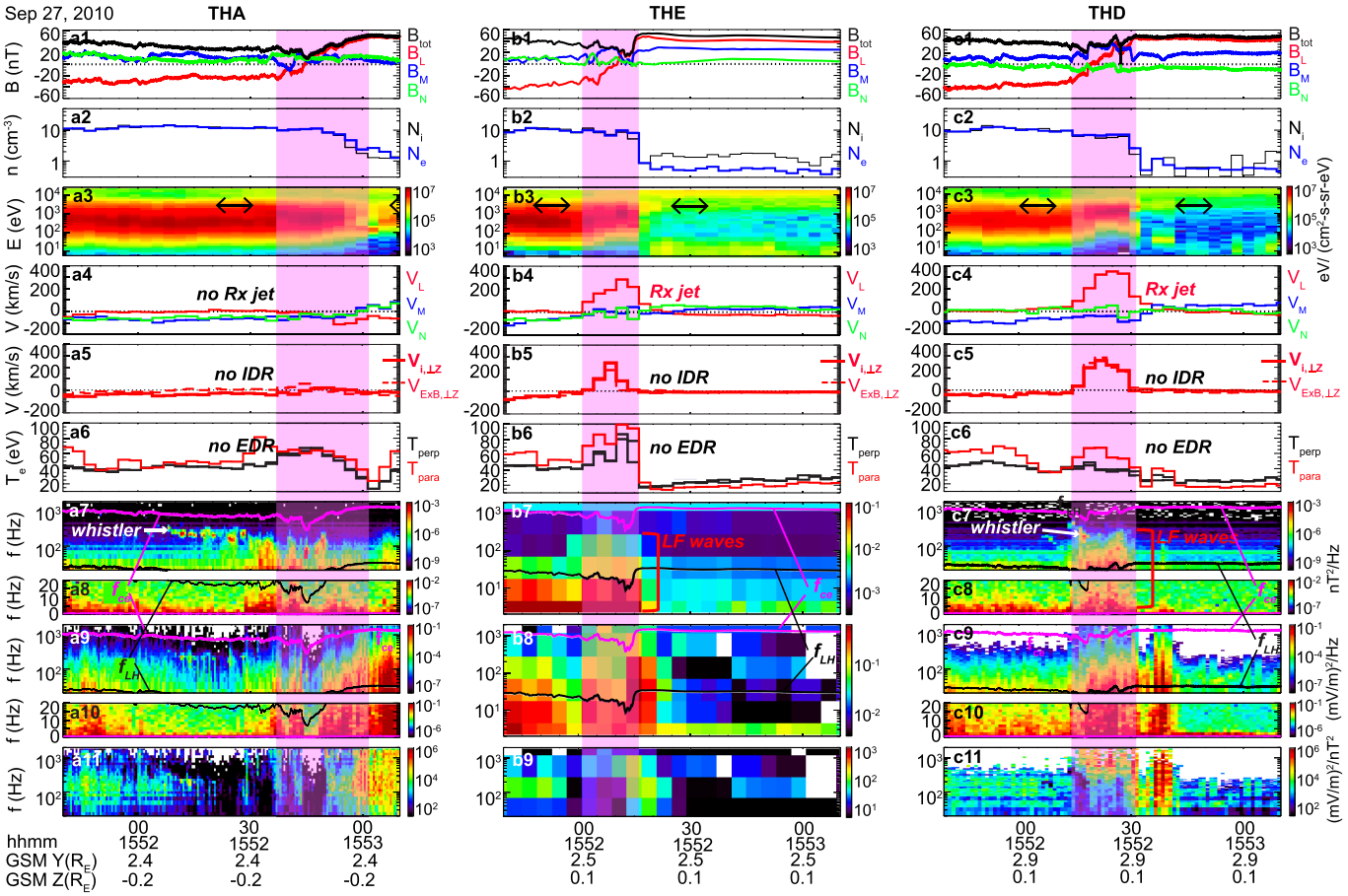

Figure 2. Panels a1–a4, b1–b4, and c1–c4: magnetic field, plasma density, ion energy spectra, and ion bulk velocity at THA, THE, and THD, respectively. The magnetic field data were taken from high-resolution FGM data for THA and THD and from low-resolution FGM data for THE. The plasma measurements were taken from burst-mode ESA data for THA and THD and reduced mode for THE. Panels a5, b5, c5: comparison of the perpendicular ion bulk velocity and the electric field drift velocity in GSM Z direction, the latter being downsampled to 3 s to be consistent with the ion bulk velocity. Panels a6, b6, c6: electron temperature taken from burst-mode ESA data for THA and THD and fast-mode ESA data for THE. Panels a7–a10, b7–b8, c7–c10: spectrograms of B_w and E_w. THA and THD measurements were computed from particle burst mode of FFT and high-resolution of FGM for B_w, and EFI for E_w. THE measurements were taken from FBK. The magenta lines mark electron gyrofrequency and the black line marks the lower hybrid frequency. Panels a11, b9, c11: the ratio of E_w to B_w.

lower hybrid frequency, and the waves were more parallel to the background magnetic field B_0 than the surrounding. Similar waveforms have been observed by Ergun *et al.* (2017) and Wilder *et al.* (2019). Although the nature of the waves is not completely understood, they are noted to differ from classic lower hybrid drift instability (LHDI) as LHDI produces electrostatic fluctuations with a wave vector that is perpendicular to $\boldsymbol{B_0}$. Ergun *et al.* (2017) found that the electromagnetic waves are consistent with a thin, oscillating current sheet that is corrugated by a surface wave near the X-line, which motivated Wilder *et al.* (2019) to name the waves as current corrugation. It is not entirely clear how far current corrugation can propagate from EDRs, but if it can propagate a long distance like LHDI (Chen *et al.,* 2017), it may be the wave mode seen by THD.

THD observations also bear similarity with kinetic Alfvén waves (KAWs) studied by Øieroset *et al.* (2014) where the waves occur in a magnetic flux rope flanked by two active reconnection X-lines. Here the KAWs extended to frequency much higher than the ion cyclotron frequency (1-2 Hz) because they were Doppler shifted when being observed in the spacecraft reference frame. However, the plasma environment in Øieroset *et al.* (2014) has a density that is more or less uniform, while the large density gradient at THD could drive ions and electrons to undergo diamagnetic drifts (Chaston *et al.,* 2005). Given the differences in the observed waves between our event and reports by others, we only refer to our observed waves as low-frequency waves without a definitive wave-mode classification.

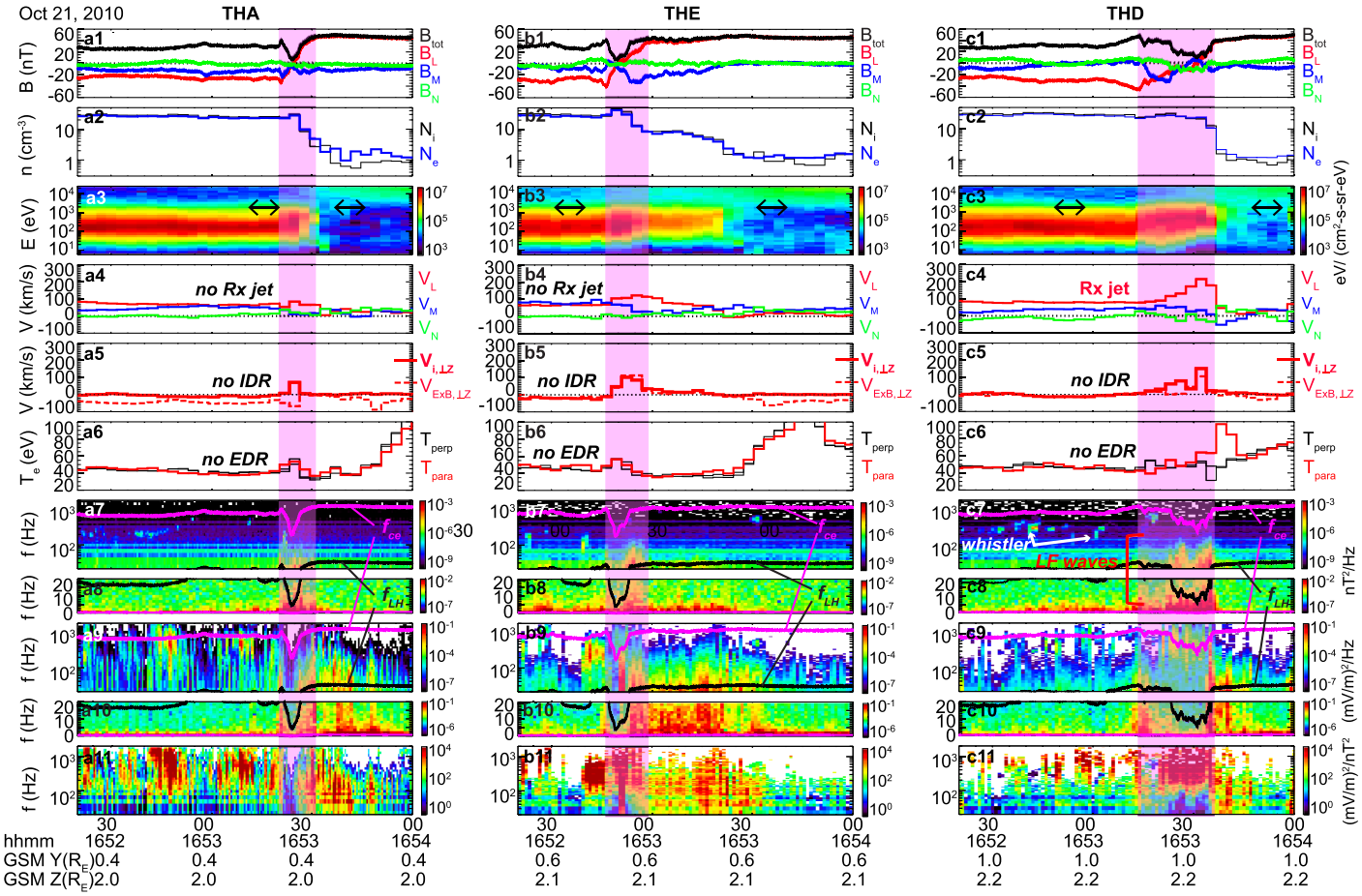

Figure 3. Similar to Figure 2 but for the event on 21 October 2010. The *N* component of the *LMN* coordinates are (0.978, −0.176, 0.111), (0.981, −0.047, 0.190), and (0.983, −0.163, 0.087) in GSM coordinates for THA, THE, and THD, respectively. All data collections of the three spacecraft were in burst mode.

In contrast, THA only observed the broadband low-frequency electromagnetic waves for a very brief interval during 15:52:38–15:52:43 UT. Although not of our main interest, THA observed a train of waves whose frequency is consistent with whistler mode wave in the magnetosheath. Whistler mode waves also occurred on the two sides of the B_0 minimum at the THA magnetopause crossing, and on the magnetosheath edge of THD crossing. THE was in not in burst mode, and the wave perturbations were obtained from filter bank (FBK) rather than fast Fourier transform (FFT) data to retain the relatively high time resolution. It captured wave enhancement below ~200 Hz across the magnetopause just like THD. Therefore, the low-frequency waves subsided from THD and THE to THA in a similar manner to the reconnection jets.

Note that low-frequency electromagnetic waves are not always present at the magnetopause. They are absent, for instance, at the non-reconnecting magnetopause (interested readers can find an example in Figure S2). The fact that the waves were not completely absent at THA in Figure 2 may suggest that reconnection at THD and THE had excited waves which spread over a broader azimuthal area than the reconnection jet. If the waves were excited locally within the reconnection jet (Lapenta *et al.,* 2014, 2018; Pucci *et al.,* 2017), they might have propagated at an angle to the jet direction.

3.1.2. Event #2

The second event occurred on 21 October 2010 as presented in Figure 3. The hybrid Alfvén speed was comparatively low, being 191 km/s, due to the higher plasma density in the magnetosheath than Event #1. Thus, the ion bulk flow upon THD magnetopause crossing (Panel c4) was Alfvénic. The flow speed was 70% of the speed of the predicted reconnection jet, and the direction differed from the predicted jet by 23°. ΔV^* was 0.65. Toward the dawn, ΔV^* was 0.36 and 0.22 at THE and THA, respectively. Neither THA nor THE observed ion bulk velocities significantly deviating from electric field drifts as expected from IDRs (Panels a5 and b5), or

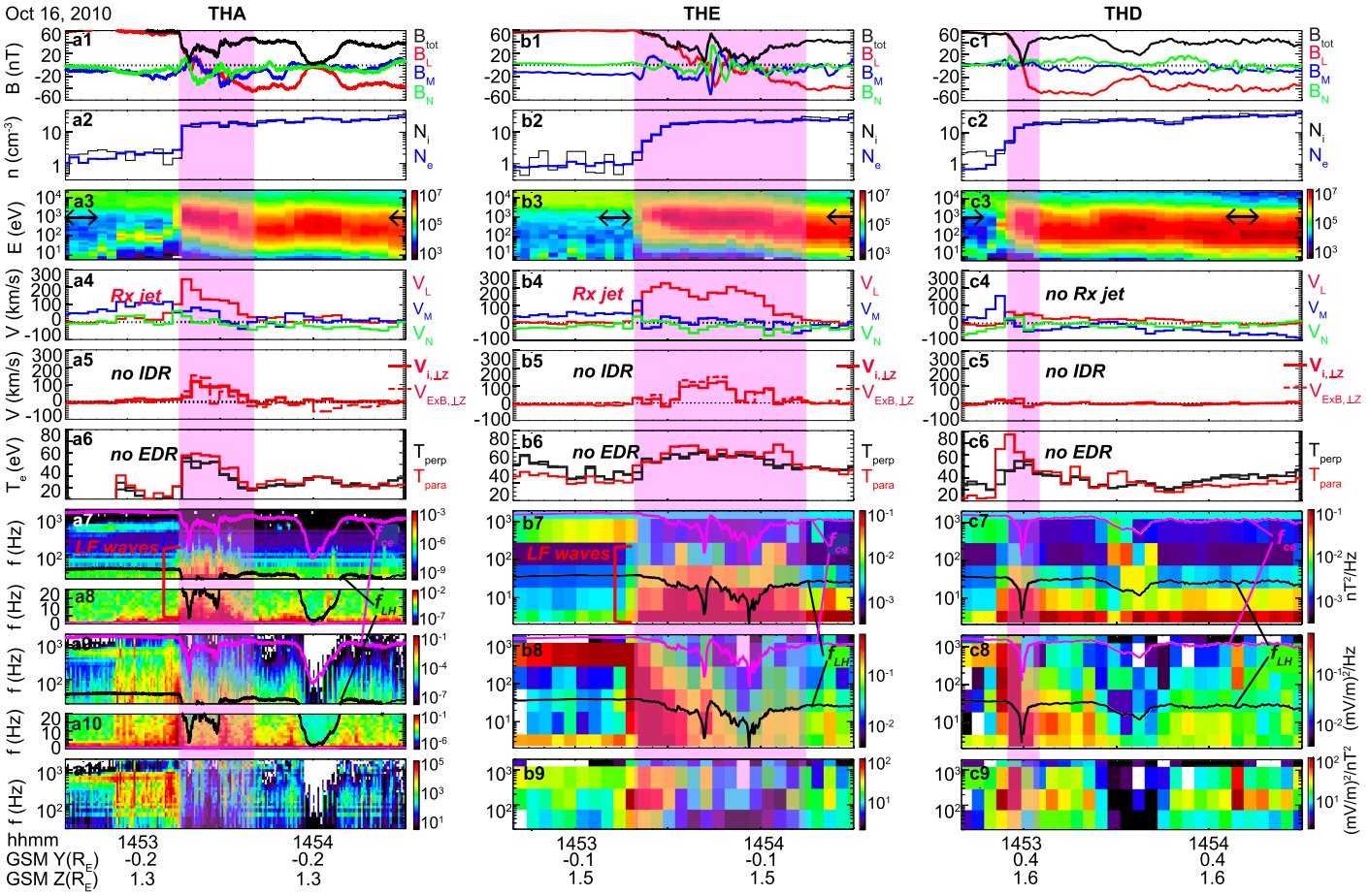

Figure 4. Similar to Figure 2 but for 16 October 2010 event. The *N* component of the *LMN* coordinates are (0.970, −0.226, 0.094), (0.962, 0.197, 0.191), and (0.920, −0.250, 0.304) in GSM coordinates for THA, THE, and THD, respectively. Only THA was in burst mode. Treatment of THE and THD data was similar to THD in Figure 2.

electron heating as expected from EDRs (Panels a6 and b6). Since the spacecraft not observing reconnection jets were again located upstream of the reconnection jet, the transition from active to inactive was not due to flow deceleration in the *L* direction but reflects a termination of reconnection activity over 0.4 R_E in the azimuthal direction.

Similar to the first event, THD observed broadband low-frequency electromagnetic waves below ~200 Hz and the bulk of B_w power spectral density was around and below the lower hybrid frequency. There existed additionally strong E_w fluctuations on the magnetosphere- and magnetosheath-side of the magnetopause, which are likely to be the classic LHDI as Wilder *et al.* (2019) pointed out. THE also detected low-frequency waves, but the intensity was weaker than that of THD, and the waves at THA were even weaker.

3.1.3. Event #3

The third event occurred on 16 October 2010 as presented in Figure 4. The reconnection features were very similar to those of the first two events, and therefore, this is another indication that it is not very rare for reconnection to terminate on spatial scales of a few tens of ion inertial lengths, although a statistical study is warranted to obtain the occurrence rate. The result is consistent with Wang *et al.* (2005) and implies that the sub-R_E scale is a critical azimuthal scale of magnetopause reconnection.

3.2. Magnetopause Conditions of the Spatially Varying Reconnection

To gain insight on why a reconnection jet was present at some of the three spacecraft and absent at others, we compare the magnetopause conditions at the three spacecraft locations. As listed in Table 1, the studied conditions include the normalized guide field, magnetic shear angle θ across the magnetopause, change of

Table 1
Magnetopause Conditions of the Studied Events

	Event 1: 2010 Sep 27			Event 2: 2010 Oct 21			Event 3: 2010 Oct 16		
	THA	THE	THD	THA	THE	THD	THA	THE	THD
$B_M/B_{L,\ \mathrm{asym}}$	0.2	**0.4**	**0.5**	0.4	0.4	**0.2**	**0.2**	**0.2**	0.1
θ (°)	146	**130**	**139**	141	161	**163**	**174**	**156**	169
$\Delta\beta$	1.5	**0.8**	**0.7**	1.1	1.3	**0.8**	**1.0**	**0.9**	0.9
$\Delta V_L/V_{\mathrm{A,asym},L}$	0.1	**0.1**	**0.1**	0.2	0.3	**0.2**	**0.0**	**0.0**	0.0
$\Delta V_M/V_{\mathrm{A,asym},L}$	0.4	**0.3**	**0.3**	0.2	0.3	**0.0**	**0.2**	**0.3**	0.3
w (s)	14	**10**	**13**	8	16	**16**	**17**	**38**	5

Note. From top to bottom are the normalized guide field, magnetic shear angle, changes in plasma beta and in ion velocity across the magnetopause, and current sheet thickness. Spacecraft that observed reconnection ion jets are shown in bold.

plasma β, change of the V_L and V_M, and thickness of the current layer. The changes across the magnetopause are determined as differences between averaged magnetosheath and magnetosphere properties, and the averages are calculated based on 10-s intervals (marked as black arrows in panels a3, b3, and c3 of Figures 2–4) adjacent to the magnetopause boundary layer. Here, we identify the boundary layer using the ion energy spectra to exclude regions with mixed magnetosheath and magnetosphere plasmas. We assume the magnetopause motion to be uniform at the spatial scale of our interest. For each event, we compare the duration of magnetopause crossings to infer the relative thickness between the three spacecraft. The duration is defined by 75% of the B_L change across the magnetopause, starting from the time when B_L reaches 12.5% of the change and ending at 87.5% of the change. Our assumption of uniform motion and our focus of relative current sheet thickness arise from the consideration that the magnetopause motion determined by single spacecraft can be far from precise (Bauer *et al.,* 2000; Haaland *et al.,* 2004) and that the de Hoffman-Teller frame, which is used to determine the motion speed, cannot be obtained at a nonreconnecting current sheet.

The guide field has been suggested to affect reconnection rate in simulations (Peng *et al.,* 2017; Pritchett & Coroniti, 2004; Ricci *et al.,* 2004; Wang *et al.,* 2000). We determine the guide field by averaging the M component of the magnetic field across the MVA interval and normalize it by the hybrid reconnecting magnetic field strength $B_{L,\ \mathrm{asym}}$, which is defined as (Birn *et al.,* 2008)

$$B_{L,\mathrm{asym}} = \sqrt{|B_{L,\mathrm{msp}}|\cdot|B_{L,\mathrm{msh}}|},$$

where $B_{L,\mathrm{msp}}$ and $B_{L,\mathrm{msh}}$ are B_L in the magnetosphere and magnetosheath, respectively. Our results show that the presence/absence of reconnection has no clear association with the normalized guide field. The change in plasma β, combined with magnetic shear angle θ, has been reported to affect occurrence of asymmetric reconnection because of the diamagnetic drift effect (Phan *et al.,* 2013; Swisdak *et al.,* 2003; 2010). Reconnection is unlikely to occur if $\Delta\beta$ is larger than a certain threshold determined by θ and a free parameter associated with the width of the plasma pressure gradient. θ varied by <20° for all three events. For Events 1 and 2, the values of $\Delta\beta$ at active reconnection sites were indeed smaller than those at inactive sites. In Event 3, however, no significant difference is found.

If the velocity shear across the magnetopause is Alfvénic, reconnection is likely to be suppressed (Cassak & Otto, 2011; Doss *et al.,* 2015; Liu *et al.,* 2018). Since the spacecraft traversed the magnetopause near the subsolar point, it is not surprising that the observed velocity shears were all sub-Alfvénic (the Alfvén speed used here is the hybrid Alfvén speed (Cassak & Shay, 2007)). The thickness of the current layer can affect the development of reconnection because tearing instability grows faster at a thin than a thick current layer. However, the observed thickness again did not show clear association with reconnection. In fact, in Event 3, the current sheet was thinnest at THA where reconnection did not occur.

Therefore, we cannot identify causes of the spatial variation of reconnection from the local parameters at the magnetopause. One may wonder whether there existed localized deformations of the magnetopause current sheet, but the hypothesis is not supported by our MVA analysis, which has produced very similar current sheet normal directions (difference < 5%) between the three spacecraft. We have not found evidence of

localized upstream drivers either, such as magnetosheath high-speed jets reported by Hietala *et al*. (2018). A statistical study should be conducted to unbiasedly confirm this lack of clear drivers, but the present finding suggests that magnetopause reconnection is likely to be intrinsically finite in space, at least at one end of the X-line and at certain stages of its development. Theories and observations have indeed suggested a spreading phase of reconnection before the X-line becomes long (Huba & Rudakov, 2002; Lapenta *et al.,* 2006; Nakamura *et al.,* 2012; Phan *et al.,* 2006; Shay *et al.,* 2003; Shepherd & Cassak, 2012; Walsh *et al.,* 2018; Zou *et al.,* 2018). Another explanation is that magnetopause conditions evolve as reconnection proceeds, and one should examine conditions right before reconnection onset time and right at the onset location to infer the causes of variation. The conditions right before the onset, however, are difficult to pinpoint because a spacecraft traverses the magnetopause as a snapshot in time, where information about conditions immediately before the traversal, or whether reconnection initiates after the traversal cannot be easily acquired.

4. Summary

We study how magnetopause reconnection varies in the azimuthal direction at sub-R_E scale, or a few to tens of ion inertial lengths. We find situations when Alfvénic reconnection jets are present at some spacecraft and absent at others that are located a few tenths of an R_E away. The absence of jets is not due to the spacecraft encountering an IDR or EDR or a magnetic flux rope flanked by two reconnection sites. Strong (weak) plasma jets are associated with strong (weak) broadband low-frequency electromagnetic waves. Causes of the variation are not directly identified from local magnetopause or upstream magnetosheath conditions, suggesting that reconnection could naturally be a finite process, at least at one end of the X-line and at certain stages of its development.

Acknowledgments
We thank Paul Cassak for the valuable discussion and suggestions. The study is supported by the NSF National Science Board (NSB) (NSF AGS-1664885). H. L. is supported by National Aeronautics and Space Administration (NASA) grant NNX16AG76G, NSF EPSCoR RII-Track-1 Cooperative Agreement OIA-1655280, and NSF/DOE Partnership in Basic Plasma Science and Engineering via NSF grant PHY-1707247. Q. M. would like to acknowledge the NASA grant 80NSSC20K0196. THEMIS mission is supported by NASA contract NAS5-02099, and the data are accessible from http://themis.ssl.berkeley.edu/. OMNI data are accessible from https://omniweb.gsfc.nasa.gov/.

References

Bauer, T. M., Dunlop, M. W., Sonnerup, B. U. O., Sckopke, N., Fazakerley, A. N., & Khrabrov, A. V. (2000). Dual spacecraft determinations of magnetopause motion. *Geophysical Research Letters*, *27*, 1835–1838. https://doi.org/10.1029/2000GL000041

Birn, J., Borovsky, J. E., & Hesse, M. (2008). Properties of asymmetric magnetic reconnection. *Physics of Plasmas*, *15*(3), 2101. https://doi.org/10.1063/1.2888491

Borovsky, J. E., Hesse, M., Birn, J., & Kuznetsova, M. M. (2008). What determines the reconnection rate at the dayside magnetosphere? *Journal of Geophysical Research*, *113*, A07210. https://doi.org/10.1029/2007JA012645

Burch, J. L., & Phan, T. D. (2016). Magnetic reconnection at the dayside magnetopause: Advances with MMS. *Geophysical Research Letters*, *43*, 8327–8338. https://doi.org/10.1002/2016GL069787

Burch, J. L., Torbert, R. B., Phan, T. D., Chen, L. J., Moore, T. E., Ergun, R. E., et al. (2016). Electron-scale measurements of magnetic reconnection in space. *Science*, *352*(6290), aaf2939. https://doi.org/10.1126/science.aaf2939

Cao, D., Fu, H. S., Cao, J. B., Wang, T. Y., Graham, D. B., Chen, Z. Z., et al. (2017). MMS observations of whistler waves in electron diffusion region. *Geophysical Research Letters*, *44*, 3954–3962. https://doi.org/10.1002/2017GL072703

Cassak, P., & Fuselier, S. A. (2015). Reconnection at Earth's dayside magnetopause. In W. Gonzalez, & E. Parker (Eds.), *Magnetic reconnection*, *Astrophysics and space science library*, (Vol. 427, pp 213-276). Heidelberg, Germany: Springer.

Cassak, P. A., & Otto, A. (2011). Scaling of the reconnection rate with anti-parallel symmetric shear flow. *Physics of Plasmas*, *18*(7), 074501. https://doi.org/10.1063/1.3609771

Cassak, P. A., & Shay, M. A. (2007). Scaling of asymmetric magnetic reconnection: General theory and collisional simulations. *Physics of Plasmas*, *14*(10), 102114. https://doi.org/10.1063/1.2795630

Chaston, C. C., Phan, T. D., Bonnell, J. W., Mozer, F. S., Acuna, M., Goldstein, M. L., et al. (2005). Drift-kinetic Alfvén waves observed near a reconnection X line in the Earth's magnetopause. *Physical Review Letters*, *95*(6), 065002. https://doi.org/10.1103/PhysRevLett.95.065002

Chen, L.-J., Hesse, M., Wang, S., Gershman, D., Ergun, R., Pollock, C., et al. (2016). Electron energization and mixing observed by MMS in the vicinity of an electron diffusion region during magnetopause reconnection. *Geophysical Research Letters*, *43*, 6036–6043. https://doi.org/10.1002/2016GL069215

Chen, Y., Toth, G., Cassak, P. A., Jia, X., Gombosi, T. I., Slavin, J., et al. (2017). Global three-dimensional simulation of Earth's dayside reconnection using a two-way coupled magnetohydrodynamics with embedded particle-in-cell model: Initial results. *Journal of Geophysical Research: Space Physics*, *122*, 10,318–10,335. https://doi.org/10.1002/2017JA024186

Chen, Z. Z., Fu, H. S., Wang, Z., Liu, C. M., & Xu, Y. (2019). Evidence of magnetic nulls in the reconnection at bow shock. *Geophysical Research Letters*, *46*, 10,209–10,218. https://doi.org/10.1029/2019GL084360

Dai, L., Wang, C., Angelopoulos, V., & Glassmeier, K.-H. (2015). In situ evidence of breaking the ion frozen-in condition via the non-gyrotropic pressure effect in magnetic reconnection. *Annales de Geophysique*, *33*, 1147–1153. https://doi.org/10.5194/angeo-33-1147-2015

Doss, C. E., Komar, C. M., Cassak, P. A., Wilder, F. D., Eriksson, S., & Drake, J. F. (2015). Asymmetric magnetic reconnection with a flow shear and applications to the magnetopause. *Journal of Geophysical Research: Space Physics*, *120*, 7748–7763. https://doi.org/10.1002/2015JA021489

Dunlop, M. W., Zhang, Q.-H., Bogdanova, Y. V., Trattner, K. J., Pu, Z., Hasegawa, H., et al. (2011). Magnetopause reconnection across wide local time. *Annales de Geophysique*, *29*, 1683–1697. https://doi.org/10.5194/angeo-29-1683-2011

Ergun, R. E., Chen, L. J., Wilder, F. D., Ahmadi, N., Eriksson, S., Usanova, M. E., et al. (2017). Drift waves, intense parallel electric fields, and turbulence associated with asymmetric magnetic reconnection at the magnetopause. *Geophysical Research Letters*, *44*, 2978–2986. https://doi.org/10.1002/2016GL072493

Fasel, G. J. (1995). Dayside poleward moving auroral forms: A statistical study. *Journal of Geophysical Research*, *100*, 11,891–11,905. https://doi.org/10.1029/95JA00854

Fear, R. C., Milan, S. E., Lucek, E. A., Cowley, S. W. H., & Fazakerley, A. N. (2010). Mixed azimuthal scales of flux transfer events. In H. Laakso, M. Taylor, & C. P. Escoubet (Eds.), *The Cluster Active Archive—Studying the Earth's space plasma environment*, *Astrophysics and Space Science Proceedings*, (pp. 389–398). Dordrecht, Netherlands: Springer. https://doi.org/10.1007/978-90-481-3499-1_27

Fu, H. S., Cao, J. B., Cao, D., Wang, Z., Vaivads, A., Khotyaintsev, Y. V., et al. (2019a). Evidence of magnetic nulls in electron diffusion region. *Geophysical Research Letters*, *46*, 48–54. https://doi.org/10.1029/2018GL080449

Fu, H. S., Cao, J. B., Khotyaintsev, Y. V., Sitnov, M. I., Runov, A., Fu, S. Y., et al. (2013a). Dipolarization fronts as a consequence of transient reconnection: In situ evidence. *Geophysical Research Letters*, *40*, 6023–6027. https://doi.org/10.1002/2013GL058620

Fu, H. S., Khotyaintsev, Y. V., Vaivads, A., Retinò, A., & André, M. (2013b). Energetic electron acceleration by unsteady magnetic reconnection. *Nature Physics*, *9*(7), 426–430. https://doi.org/10.1038/NPHYS2664

Fu, H. S., Vaivads, A., Khotyaintsev, Y. V., André, M., Cao, J. B., Olshevsky, V., et al. (2017). Intermittent energy dissipation by turbulent reconnection. *Geophysical Research Letters*, *44*, 37–43. https://doi.org/10.1002/2016GL071787

Fu, H. S., Vaivads, A., Khotyaintsev, Y. V., Olshevsky, V., André, M., Cao, J. B., et al. (2015). How to find magnetic nulls and reconstruct field topology with MMS data? *Journal of Geophysical Research: Space Physics*, *120*, 3758–3782. https://doi.org/10.1002/2015JA021082

Fu, H. S., Xu, Y., Vaivads, A., & Khotyaintsev, Y. V. (2019b). Super-efficient electron acceleration by an isolated magnetic reconnection. *Astrophysical Journal Letters*, *870*(2), L22. https://doi.org/10.3847/2041-8213/aafa75

Genestreti, K. J., Burch, J. L., Cassak, P. A., Torbert, R. B., Ergun, R. E., Varsani, A., et al. (2017). The effect of a guide field on local energy conversion during asymmetric magnetic reconnection: MMS observations. *Journal of Geophysical Research: Space Physics*, *122*, 11,342–11,353. https://doi.org/10.1002/2017JA024247

Genestreti, K. J., Varsani, A., Burch, J. L., Cassak, P. A., Torbert, R. B., Nakamura, R., et al. (2018). MMS observation of asymmetric reconnection supported by 3-D electron pressure divergence. *Journal of Geophysical Research: Space Physics*, *123*, 1806–1821. https://doi.org/10.1002/2017JA025019

Haaland, S., Sonnerup, B., Dunlop, M., Balogh, A., Georgescu, E., Hasegawa, H., et al. (2004). Four-spacecraft determination of magnetopause orientation, motion and thickness: Comparison with results from single-spacecraft methods. *Annales Geophysicae*, *22*(4), 1347–1365. https://doi.org/10.5194/angeo-22-1347-2004

Hasegawa, H., Kitamura, N., Saito, Y., Nagai, T., Shinohara, I., Yokota, S., et al. (2016). Decay of mesoscale flux transfer events during quasi-spatially extended reconnection at the magnetopause. *Geophysical Research Letters*, *43*, 4755–4762. https://doi.org/10.1002/2016GL069225

Hietala, H., Phan, T. D., Angelopoulos, V., Oieroset, M., Archer, M. O., Karlsson, T., & Plaschke, F. (2018). In situ observations of a magnetosheath high-speed jet triggering magnetopause reconnection. *Geophysical Research Letters*, *45*, 1732–1740. https://doi.org/10.1002/2017GL076525

Huba, J. D., & Rudakov, L. I. (2002). Three-dimensional Hall magnetic reconnection. *Physics of Plasmas*, *9*(11), 4435–4438. https://doi.org/10.1063/1.1514970

Hudson, P. D. (1970). Discontinuities in an anisotropic plasma and their identification in the solar wind. *Planetary and Space Science*, *18*(11), 1611–1622. https://doi.org/10.1016/0032-0633(70)90036-X

Kan, J. R. (1988). A theory of patchy and intermittent reconnections for magnetospheric flux transfer events. *Journal of Geophysical Research*, *93*, 5613–5623. https://doi.org/10.1029/JA093iA06p05613

Kuo, H., Russell, C. T., & Le, G. (1995). Statistical studies of flux transfer events. *Journal of Geophysical Research*, *100*, 3513–3519. https://doi.org/10.1029/94JA02498

Lapenta, G., Goldman, M., Newman, D., Markidis, S., & Divin, A. (2014). Electromagnetic energy conversion in downstream fronts from three dimensional kinetic reconnection. *Physics of Plasmas*, *21*(5), 055702. https://doi.org/10.1063/1.4872028

Lapenta, G., Krauss-Varban, D., Karimabadi, H., Huba, J. D., Rudakov, L. I., & Ricci, P. (2006). Kinetic simulations of X-line expansion in 3D reconnection. *Geophysical Research Letters*, *33*, L10102. https://doi.org/10.1029/2005GL025124

Lapenta, G., Pucci, F., Olshevsky, V., Servidio, S., Sorriso-Valvo, L., Newman, D. L., & Goldman, M. V. (2018). Nonlinear waves and instabilities leading to secondary reconnection in reconnection outflows. *Journal of Plasma Physics*, *84*(1), 715840103. https://doi.org/10.1017/S002237781800003X

Li, T.-C., Liu, Y., Hesse, M., & Zou, Y. (2020). Three-dimensional X-line Spreading in Asymmetric Magnetic Reconnection. *Journal of Geophysical Research: Space Physics*, *125*, e2019JA027094. https://doi.org/10.1029/2019ja027094

Liu, Y.-H., Hesse, M., Guo, F., Li, H., & Nakamura, T. K. M. (2018). Strongly localized magnetic reconnection by the super-Alfvénic shear flow. *Physics of Plasmas*, *25*(8), 080701. https://doi.org/10.1063/1.5042539

Liu, Y.-H., Li, T. C., Hesse, M., Sun, W.-J., Liu, J., Burch, J., et al. (2019). Three-dimensional magnetic reconnection with a spatially confined X-line extent: Implications for dipolarizing flux bundles and the dawn-dusk asymmetry. *Journal of Geophysical Research: Space Physics*, *124*, 2819, 2019JA026539–2830. https://doi.org/10.1029/2019JA026539

McWilliams, K. A., Yeoman, T. K., & Provan, G. (2000). A statistical survey of dayside pulsed ionospheric flows as seen by the CUTLASS Finland HF radar. *Annales de Geophysique*, *18*(4), 445–453. https://doi.org/10.1007/s00585-000-0445-8

Meyer, J. C. (2015). Structure of the diffusion region in three dimensional magnetic reconnection (PhD thesis), University of Delaware.

Mozer, F. S., Bale, S. D., & Phan, T. D. (2002). Evidence of diffusion regions at a subsolar magnetopause crossing. *Physical Review Letters*, *89*(1), 015002. https://doi.org/10.1103/PhysRevLett.89.015002

Nakamura, T. K. M., Nakamura, R., Alexandrova, A., Kubota, Y., & Nagai, T. (2012). Hall magnetohydrodynamic effects for three-dimensional magnetic reconnection with finite width along the direction of the current. *Journal of Geophysical Research*, *117*, A03220. https://doi.org/10.1029/2011JA017006

Nishida, A. (1989). Can random reconnection on the magnetopause produce the low latitude boundary layer? *Geophysical Research Letters*, *61*, 227–230. https://doi.org/10.1029/GL016i003p00227

Øieroset, M., Sundkvist, D., Chaston, C. C., Phan, T. D., Mozer, F. S., McFadden, J. P., et al. (2014). Observations of plasma waves in the colliding jet region of amagnetic flux rope flanked by two active X lines at the subsolar magnetopause. *Journal of Geophysical Research: Space Physics*, *119*, 6256–6272. https://doi.org/10.1002/2014JA020124

Paschmann, G., Papamastorakis, I., Baumjohann, W., Sckopke, N., Carlson, C. W., Sonnerup, B. U., & Lühr, H. (1986). The magnetopause for large magnetic shear: AMPTE/IRM observations. *Journal of Geophysical Research*, *91*, 11,099–11,115. https://doi.org/10.1029/JA091iA10p11099

Paschmann, G., Papamastorakis, I., Sckopke, N., Haerendel, G., Sonnerup, B. U. O., Bame, S. J., et al. (1979). Plasma acceleration at the Earth's magnetopause: Evidence for magnetic reconnection. *Nature*, *282*, 243–246. https://doi.org/10.1038/282243a0

Peng, F. Z., Fu, H. S., Cao, J. B., Graham, D. B., Chen, Z. Z., Cao, D., et al. (2017). Quadrupolar pattern of the asymmetric guide-field reconnection. *Journal of Geophysical Research: Space Physics*, *122*, 6349–6356. https://doi.org/10.1002/2016JA023666

Phan, T. D., Eastwood, J. P., Cassak, P. A., Øieroset, M., Gosling, J. T., Gershman, D. J., et al. (2016). MMS observations of electron-scale filamentary currents in the reconnection exhaust and near the X line. *Geophysical Research Letters*, *43*, 6060–6069. https://doi.org/10.1002/2016GL069212

Phan, T. D., Hasegawa, H., Fujimoto, M., Oieroset, M., Mukai, T., Lin, R. P., & Paterson, W. R. (2006). Simultaneous Geotail and Wind observations of reconnection at the subsolar and tail flank magnetopause. *Geophysical Research Letters*, *33*, L09104. https://doi.org/10.1029/2006GL025756

Phan, T. D., Kistler, L. M., Klecker, B., Haerendel, G., Paschmann, G., Sonnerup, B. U. Ö., et al. (2000). Extended magnetic reconnection at the Earth's magnetopause from detection of bi-directional jets. *Nature*, *404*(6780), 848–850. https://doi.org/10.1038/35009050

Phan, T. D., & Paschmann, G. (1996). Low-dayside magnetopause and boundary layer for high magnetic shear: 1. Structure and motion. *Journal of Geophysical Research*, *101*, 7801–7815. https://doi.org/10.1029/95JA03752

Phan, T. D., Paschmann, G., Gosling, J. T., Oieroset, M., Fujimoto, M., Drake, J. F., & Angelopoulos, V. (2013). The dependence of magnetic reconnection on plasma β and magnetic shear: Evidence from magnetopause observations. *Geophysical Research Letters*, *40*, 11–16. https://doi.org/10.1029/2012GL054528

Pritchett, P. L., & Coroniti, F. V. (2001). Kinetic simulations of 3-D reconnection and magnetotail disruptions. *Earth, Planets and Space*, *53*(6), 635–643. https://doi.org/10.1186/BF03353283

Pritchett, P. L., & Coroniti, F. V. (2004). Three-dimensional collisionless magnetic reconnection in the presence of a guide field. *Journal of Geophysical Research*, *109*, A01220. https://doi.org/10.1029/2003JA009999

Pucci, F., Servidio, S., Sorriso-Valvo, L., Olshevsky, V., Matthaeus, W. H., Malara, F., et al. (2017). Properties of turbulence in the reconnection exhaust: Numerical simulations compared with observations. *The Astrophysical Journal*, *841*(1), 60. https://doi.org/10.3847/1538-4357/aa704f

Ricci, P., Brackbill, J. U., Daughton, W., & Lapenta, G. (2004). Collisionless magnetic reconnection in the presence of a guide field. *Physics of Plasmas*, *11*(8), 4102–4114. https://doi.org/10.1063/1.1768552

Scurry, L., Russell, C. T., & Gosling, J. T. (1994). Geomagnetic activity and the beta dependence of the dayside reconnection rate. *Journal of Geophysical Research*, *99*, 14,811–14,814. https://doi.org/10.1029/94JA00794

Shay, M. A., Drake, J. F., Swisdak, M., Dorland, W., & Rogers, B. N. (2003). Inherently three dimensional magnetic reconnection: A mechanism for bursty bulk flows? *Geophysical Research Letters*, *30*(6), 1345. https://doi.org/10.1029/2002GL016267

Shepherd, L. S., & Cassak, P. A. (2012). Guide field dependence of 3-D X-line spreading during collisionless magnetic reconnection. *Journal of Geophysical Research*, *117*, A10101. https://doi.org/10.1029/2012JA017867

Swisdak, M., Opher, M., Drake, J. F., & Alouani Bibi, F. (2010). The vector direction of the interstellar magnetic field outside the heliosphere. *The Astrophysical Journal*, *710*(2), 1769–1775. https://doi.org/10.1088/0004-637X/710/1769

Swisdak, M., Rogers, B. N., Drake, J. F., & Shay, M. A. (2003). Diamagnetic suppression of component magnetic reconnection at the magnetopause. *Journal of Geophysical Research*, *108*(A5), 1218. https://doi.org/10.1029/2002JA009726

Tang, X., Cattell, C., Dombeck, J., Dai, L., Wilson, L. B., Breneman, A., & Hupach, A. (2013). THEMIS observations of the magnetopause electron diffusion region: Large amplitude waves and heated electrons. *Geophysical Research Letters*, *40*, 2884–2890. https://doi.org/10.1002/grl.50565

Torbert, R. B., Burch, J. L., Argall, M. R., Alm, L., Farrugia, C. J., Forbes, T. G., et al. (2017). Structure and dissipation characteristics of an electron diffusion region observed by MMS during a rapid, normal-incidence magnetopause crossing. *Journal of Geophysical Research: Space Physics*, *122*, 11,901–11,916. https://doi.org/10.1002/2017JA024579

Trattner, K. J., Burch, J. L., Cassak, P. A., Ergun, R., Eriksson, S., Fuselier, S. A., et al. (2018). The transition between antiparallel and component magnetic reconnection at Earth's dayside magnetopause. *Journal of Geophysical Research: Space Physics*, *123*, 10,177–10,188. https://doi.org/10.1029/2018JA026081

Trattner, K. J., Mulcock, J. S., Petrinec, S. M., & Fuselier, S. A. (2007). Probing the boundary between antiparallel and component reconnection during southward interplanetary magnetic field conditions. *Journal of Geophysical Research*, *112*, A08210. https://doi.org/10.1029/2007JA012270

Trattner, K. J., Petrinec, S. M., Fuselier, S. A., & Phan, T. D. (2012). The location of reconnection at the magnetopause: Testing the maximum magnetic shear model with THEMIS observations. *Journal of Geophysical Research*, *117*, A01201. https://doi.org/10.1029/2011JA016959

Trenchi, L., Marcucci, M. F., Pallocchia, G., Consolini, G., Bavassano Cattaneo, M. B., Di Lellis, A. M., et al. (2008). Occurrence of reconnection jets at the dayside magnetopause: Double Star observations. *Journal of Geophysical Research*, *113*, A07S10. https://doi.org/10.1029/2007JA012774

Walsh, B. M., Foster, J. C., Erickson, P. J., & Sibeck, D. G. (2014b). Simultaneous ground- and space-based observations of the plasmaspheric plume and reconnection. *Science*, *343*(6175), 1122–1125. https://doi.org/10.1126/science.1247212

Walsh, B. M., Komar, C. M., & Pfau-Kempf, Y. (2017). Spacecraft measurements constraining the spatial extent of a magnetopause reconnection X line. *Geophysical Research Letters*, *44*, 3038–3046. https://doi.org/10.1002/2017GL073379

Walsh, B. M., Phan, T. D., Sibeck, D. G., & Souza, V. M. (2014a). The plasmaspheric plume and magnetopause reconnection. *Geophysical Research Letters*, *41*, 223–228. https://doi.org/10.1002/2013GL058802

Walsh, B. M., Welling, D. T., Zou, Y., & Nishimura, Y. (2018). A maximum spreading speed for magnetopause reconnection. *Geophysical Research Letters*, *45*, 5268–5273. https://doi.org/10.1029/2018GL078230

Wang, X., Bhattacharjee, A., & Ma, Z. W. (2000). Collisionless reconnection: Effects of Hall current and electron pressure gradient. *Journal of Geophysical Research*, *105*, 27,633–27,648. https://doi.org/10.1029/1999JA000357

Wang, Y. L., Elphic, R. C., Lavraud, B., Taylor, M. G. G. T., Birn, J., Raeder, J., et al. (2005). Initial results of high-latitude magnetopause and low-latitude flank flux transfer events from 3 years of Cluster observations. *Journal of Geophysical Research*, *110*, A11221. https://doi.org/10.1029/2005JA011150

Wang, Z., Fu, H. S., Liu, C. M., Liu, Y. Y., Cozzani, G., Giles, B. L., et al. (2019). Electron distribution functions around a reconnection X-line resolved by the FOTE method. *Geophysical Research Letters*, *46*(3), 1195–1204. https://doi.org/10.1029/2018GL081708

Wilder, F. D., Ergun, R. E., Hoilijoki, S., Webster, J., Argall, M. R., Ahmadi, N., et al. (2019). A survey of plasma waves appearing near dayside magnetopause electron diffusion region events. *Journal of Geophysical Research: Space Physics*, *124*, 7837–7849. https://doi.org/10.1029/2019JA027060

Xu, Y., Fu, H. S., Norgren, C., Hwang, K.-J., & Liu, C. M. (2018). Formation of dipolarization fronts after current sheet thinning. *Physics of Plasmas*, *25*(7), 072123. https://doi.org/10.1063/1.5030200

Zou, Y., Walsh, B. M., Nishimura, Y., Angelopoulos, V., Ruohoniemi, J. M., McWilliams, K. A., & Nishitani, N. (2018). Spreading speed of magnetopause reconnection X-lines using ground-satellite coordination. *Geophysical Research Letters*, *45*, 80–89. https://doi.org/10.1002/2017GL075765

Zou, Y., Walsh, B. M., Nishimura, Y., Angelopoulos, V., Ruohoniemi, J. M., McWilliams, K. A., & Nishitani, N. (2019). Local time extent of magnetopause reconnection using space–ground coordination. *Annales de Geophysique*, *37*, 215–234. https://doi.org/10.5194/angeo-37-215-2019